doi:10.1088/2041-8205/730/2/L37

UNNOTICED MAGNETIC FIELD OSCILLATIONS IN THE VERY QUIET SUN REVEALED BY SUNRISE/IMaX

M. J. Martínez González[1,2], A. Asensio Ramos[1,2], R. Manso Sainz[1,2], E. Khomenko[1,2], V. Martínez Pillet[1,2],
S. K. Solanki[3,4], A. López Ariste[5], W. Schmidt[6], P. Barthol[3], and A. Gandorfer[3]

[1] Instituto de Astrofísica de Canarias, C/Vía Láctea s/n, 38200 La Laguna, Tenerife, Spain
[2] Departamento de Astrofísica, Univ. de La Laguna, 38205, La Laguna, Tenerife, Spain
[3] Max-Planck-Institut für Sonnensystemforschung, 37191, Katlenburg-Lindau, Germany
[4] School of Space Research, Kyung Hee University, Yongin, Gyeonggi 446-701, Republic of Korea
[5] THEMIS-CNRS UPS 853, C/Vía Láctea s/n 38205, La Laguna, Tenerife, Spain
[6] Kiepenheuer-Institut für Sonnenphysik, Schöneckstr. 6, 79104 Freiburg, Germany

ABSTRACT

We present observational evidence for oscillations of magnetic flux density in the quiet areas of the Sun. The majority of magnetic fields on the solar surface have strengths of the order of or lower than the equipartition field (300–500 G). This results in a myriad of magnetic fields whose evolution is largely determined by the turbulent plasma motions. When granules evolve they squash the magnetic field lines together or pull them apart. Here, we report on the periodic deformation of the shapes of features in circular polarization observed at high resolution with SUNRISE. In particular, we note that the area of patches with a constant magnetic flux oscillates with time, which implies that the apparent magnetic field intensity oscillates in antiphase. The periods associated with this oscillatory pattern are compatible with the granular lifetime and change abruptly, which suggests that these oscillations might not correspond to characteristic oscillatory modes of magnetic structures, but to the forcing by granular motions. In one particular case, we find three patches around the same granule oscillating in phase, which means that the spatial coherence of these oscillations can reach 1600 km. Interestingly, the same kind of oscillatory phenomenon is also found in the upper photosphere.

Key words: Sun: oscillations

Online-only material: color figures

1. THE MAGNETICALLY, DYNAMICALLY ACTIVE QUIET SUN

As we enhance the spatial resolution and sensitivity of spectropolarimetric measurements, it becomes increasingly evident that magnetic fields permeate the whole quiet Sun (Orozco Suárez et al. 2007; Martínez González et al. 2008; Lites et al. 2008; Danilovic et al. 2010). The observed Zeeman polarization signals in the quietest areas of the Sun are highly dynamic, having timescales compatible with the granulation (Lin & Rimmele 1999; Harvey et al. 2007; Danilovic et al. 2010). These weak magnetic flux concentrations emerge somewhat preferentially in granules, where plasma motions are more favorable for the magnetic fields to rise across the solar atmosphere (Martínez González et al. 2007; Centeno et al. 2007; Orozco Suárez et al. 2008; Martínez González & Bellot Rubio 2009; Gömöry et al. 2010; Danilovic et al. 2010). In many of these features, the field is organized in the form of Ω-shaped loops and survives convective motions, the footpoints of these loops being passively advected by granular motions (Martínez González & Bellot Rubio 2009; Manso Sainz et al. 2010). Importantly, some of these small-scale loops do reach higher layers, at least the lower chromosphere, hence linking the very quiet photosphere to chromospheric magnetism (Martínez González & Bellot Rubio 2009; Martínez González et al. 2010; Wiegelmann et al. 2010).

In this Letter, we present another interesting feature of the small-scale solar magnetism. We find that both the area and the magnetic flux density of circular polarization patches display quasi-periodic oscillations at a constant magnetic flux.

Oscillations of line-of-sight velocity and brightness of small-scale magnetic features in solar network, faculae, and plage areas have been detected by, e.g., Lites et al. (1993), Krijger et al. (2001), De Moortel et al. (2002), De Pontieu et al. (2003),

Centeno et al. (2009), Bloomfield et al. (2006), Vecchio et al. (2009), and Jess et al. (2009). However, a clear detection of magnetic field oscillations remains elusive. Recently, Fujimura & Tsuneta (2009) used *Hinode* spectropolarimetric data with a spatial resolution of $0''.32$, showing evidence of magnetic flux oscillations, interpreted by these authors as an indication for magnetoacoustic "sausage" and "kink" modes in individual elements of plages and pores. Very little (if anything) is known about possible oscillations of magnetic features in solar internetwork areas, with much less magnetic flux. Due to the usually low amplitude of the polarization signals, the observations necessary to study the temporal behavior of small-scale patches in the internetwork are rather demanding. Here, we make use of the superb quality of the SUNRISE/IMaX data and show that magnetic fields outside active regions also oscillate, representing the first evidence for magnetic field oscillations in the quiet-Sun internetwork areas.

2. THE IMaX DATA

We analyze disk center quiet-Sun observations obtained with the IMaX instrument (Martínez Pillet et al. 2011) on board the SUNRISE balloon-borne observatory (Barthol et al. 2011; Solanki et al. 2010). The IMaX instrument is a Fabry–Pérot interferometer with polarimetric capabilities at the Fe I line at 5250.2 Å. The observational sequence consists of five filtergrams taken at ± 40, ± 80, and $+227$ mÅ from the Fe I 5250.2 Å line center. The field of view is $46''.8 \times 46''.8$, with a cutoff frequency of $(0''.15$–$0''.18)^{-1}$, the pixel size being $0''.05$. We analyze two time series of about 23 and 40 minutes duration with a cadence of about 32 s and a noise level of $\sigma = 10^{-3}$ and 7×10^{-4} I_c in the circular and linear polarization (I_c being the continuum intensity).
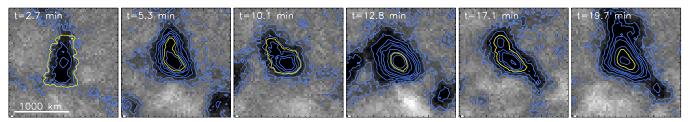
Figure 1. Time evolution of a weak circular polarization patch (corresponding to the top right panel of Figure 3). The black and white background represents the magnetic flux density computed in the weak-field approximation, saturated to ± 20 Mx cm^{-2}. Blue lines represent iso-magnetic flux densities of -130, -100, -75, -50, -40, -30, -20, -10, and -5 Mx cm^{-2}. Yellow line is the iso-magnetic flux density contour containing a time-constant magnetic flux of -4.5×10^{16} Mx.

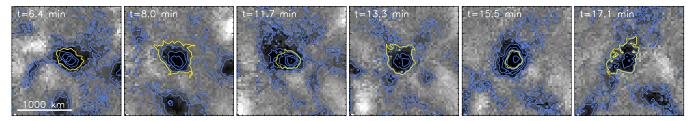(A color version of this figure is available in the online journal.)

Figure 2. Same as Figure 1 for the top left panel of Figure 3. Yellow line is the iso-magnetic flux density contour containing a time-constant magnetic flux of -5×10^{16} Mx.

(A color version of this figure is available in the online journal.)

We analyze the IMaX data before the phase-diversity reconstruction process, due to their lower noise level. The Fe I line at 5250.2 Å is a forbidden but resonant line and thus is extremely sensitive to the local temperature of the plasma (e.g., Stenflo et al. 1987; Lagg et al. 2010). We use the flux density (ϕ in Mx cm^{-2}) derived from the weak-field approximation instead of the directly observed Stokes V signal. The weak-field approximation states that the Stokes V profile is proportional to the derivative of the intensity profile and to the magnetic flux density. Taking into account the simultaneous information contained in the intensity and the Stokes V profile, we can decouple the thermodynamical and the magnetic effects. The magnetic flux density is estimated following a least-squares minimization (see M. J. Martínez González et al. 2011, in preparation). It can be expressed as

$$\phi = -\frac{\sum_i \frac{\partial I}{\partial \lambda_i} V_i}{C \sum_i \left(\frac{\partial I}{\partial \lambda_i}\right)^2}, \quad (1)$$

which uses all the wavelength samples across the profile (index i) and is therefore more accurate than determinations based on single magnetogram measurements. The constant C is defined as $4.6686 \times 10^{-13} \lambda_0^2 \bar{g}$, with λ_0 being the central wavelength (in Å) and $\bar{g}$ the effective Landé factor of the transition. The derivatives of the intensity profile have been computed numerically using the observed data. For this kind of IMaX data, this approximation is valid for magnetic fields up to ~1 kG. The estimated error is $\sigma_B = 4$ Mx cm^{-2}. If we assume that the magnetic fields are resolved (filling factor is one), Equation (1) gives the longitudinal magnetic field strength in G.
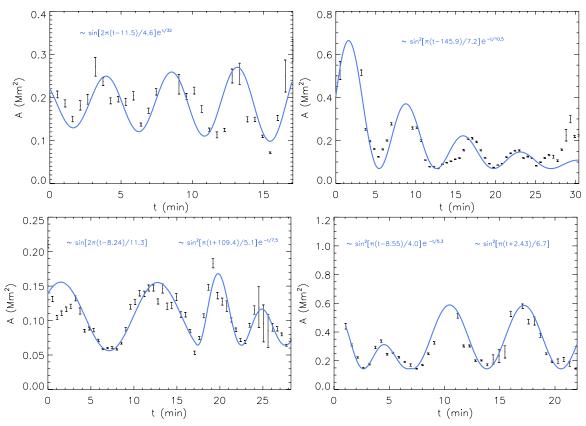
3. OSCILLATIONS OF QUIET-SUN MAGNETIC FIELDS

We focus on the temporal evolution of circular polarization patches. Magnetic patches are passively buffeted by granular motions and interact with them, fragmenting, mixing with patches of opposite or equal polarity, and canceling. This behavior has also been observed at lower spatial resolution (e.g., Martin 1988), but at higher resolution we observe more

polarization patches and hence a large probability of interaction. In fact, we estimate that roughly 50% of the circular polarization signals suffer at least one encounter with a neighboring patch in 5 minutes.

The spatial resolution of the IMaX data (~0.″15) allows us to observe an interesting dynamic property of the weak quiet-Sun polarization patches. The signals are found to vary in shape, i.e., the area enclosed in a contour containing a constant magnetic flux changes with time. This can be seen in Figures 1 and 2, following the yellow contours. Both the area and the shape clearly change with time.

Although this behavior is common to all magnetic flux density patches (the ones with significant spatial coherency), we select some particular examples to study the area fluctuations in detail. We study four low-flux patches (10^{16}–10^{17} Mx) that do not interact with another patch during the whole sequence or for a long time (at least at our present noise level) and an intense patch (10^{18} Mx). We follow the time evolution of these patches at a constant magnetic flux. In other words, the patch is defined as the signal enclosed in the magnetic flux density contour for which the magnetic flux is constant with time. At all times, the contour value is above 8 Mx cm^{-2}, which is twice the noise level of the magnetogram. The areas are enclosed in contours that are treated as polygons, hence, we increase the precision on the computation. Since the magnetic flux density has an associated error, the contours (and the areas) have also an uncertainty. We have estimated the errors associated with the areas numerically using a Monte Carlo approach. The larger the area the smaller the relative error. In our case, the errors range between 1% and 8%. These uncertainties have been propagated as Gaussian variables to derived quantities, such as the mean magnetic flux density enclosed in an area.

Figure 3 shows the time dependence of the area of four selected weak magnetic features that show clear periodic fluctuations of the area. The area fluctuates between a factor of seven and a factor of two. The four selected cases present a large variety of behaviors. From the top left, clockwise, the modes are amplified, damped, and showing two different periods and

Figure 3. Evolution of the area of four selected magnetic patches. Constant amounts of magnetic flux are followed in time, being -4.5×10^{16}, -1.0×10^{17}, 5×10^{16}, and -9×10^{16} Mx from the top left panel to the bottom right one. The measured areas are represented as error bars. The blue lines are analytical fits (using a least-squares estimator) to facilitate recognition of the quasi-periodic pattern. The time t in these expressions is given in minutes.

(A color version of this figure is available in the online journal.)

different damping or amplification factors. The periods range between 4 and 11 minutes, showing that there is not a characteristic period for these oscillatory patterns. These periods have been obtained using analytical fits to the area oscillation since the duration of these events does not allow a reliable Fourier analysis. The corresponding antiphase oscillations of the magnetic flux density have peak to peak variations from 12 up to 100 Mx cm^{-2} around the mean value, which are -24, -67, 48, and -34 Mx cm^{-2} from the top left of Figure 3, clockwise.

Figure 4 shows the area oscillations of a more intense patch (with a maximum value of 270 Mx cm^{-2}) at three different radii from the center of the structure, defined by the amount of flux contained within the considered perimeter. As for the weaker flux patches, the oscillation contains several periods. In this case, 3 and 5 minutes are the most evident. The area oscillation maintains period and phase over different fluxes, while its amplitude increases as we move away from the center of the patch. The fluctuation of the area relative to its mean value ranges from 14% to 24% from the most central to the most peripheral contour, i.e., the areas containing 1×10^{17} and 1×10^{18} Mx, respectively. The magnitude of the fluctuation of the magnetic flux density remains constant. This means that the variation of this quantity across the structure is very smooth.

The line-of-sight velocity, the continuum, and the core intensity oscillate too, showing the characteristic pattern of the p-modes, with a 5 minute period. The continuum and core intensity fluctuations exhibit a phase shift of $180°$. The velocity is also in antiphase with the continuum intensity. After removing the effect of p-modes using a subsonic filter, the speed of

sound being 4 km s^{-1}. Neither the oscillation of the velocity, the continuum, nor the core intensity seem to be related to the magnetic flux density (and area) fluctuations, as can be seen by camparing Figures 3 and 5.

Whereas some of the oscillations in area we observe display periods in the range of the p-modes, others have distinctly longer periods, even up to 11 minutes, and show an abrupt change of the wave period at a given time. Moreover, we find that the area of some magnetic patches located close together oscillate in phase. In one particular case, the co-oscillating flux patches surround a granule, the mean distance between them being about 1600 km.

4. DISCUSSION

We have shown that the magnetic field in the quiet Sun oscillates with a variety of periods compatible with the granular lifetime. These oscillations can be strongly damped (top right panel of Figure 3) or amplified (top left panel of Figure 3) with a damping time of $\sim$5–30 minutes. We have also observed that the period of the oscillation can change abruptly in the course of the time series. This would suggest that either the characteristic modes of the structure vary due to changes in their physical properties (density, magnetic field orientation, sub-resolution structure, etc.) or that they are not characteristic modes of oscillation at all.

Theoretical studies of the characteristic oscillation modes of thin flux tubes (for example the classical work by Edwin & Roberts 1983) suggest a dependence of the oscillation period on the structure size a multiplied by the wave number k, in a sense
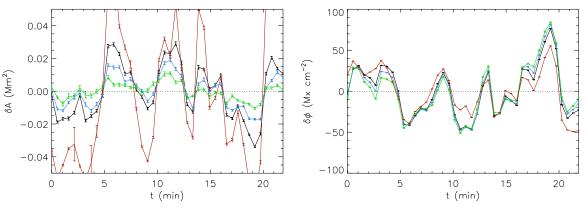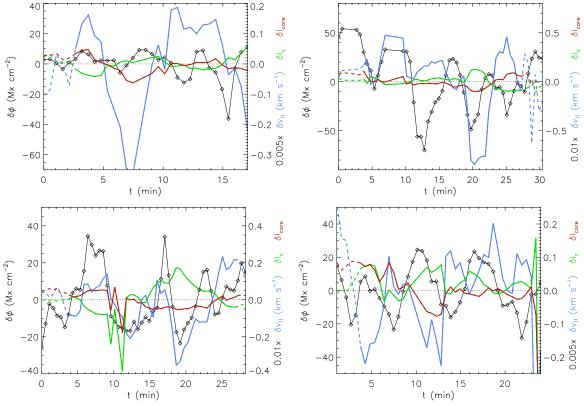
3

Figure 4. Evolution of the area (left) and magnetic flux density (right) of an intense patch (with a maximum value of 270 Mx cm^{-2}). The red line contain 1×10^{18} Mx. Note that the oscillation in area of the red line has been divided by 4. The black line represent the fluctuation of the area that contains a constant magnetic flux of 3×10^{17} Mx. The blue and green lines are the areas containing 2×10^{17} and 1×10^{17} Mx, respectively. The larger the flux (area) the further the contour lies from the center of the structure, which is defined as the position of the maximum flux density.

(A color version of this figure is available in the online journal.)

Figure 5. Evolution of diverse physical quantities of the four patches of Figure 4. The black lines represent the oscillation of the magnetic flux density with respect to its time average. Blue, green, and red lines represent the variation of the line-of-sight velocity, continuum, and core intensity with respect to its mean value, respectively. Note that these three last quantities have been multiplied by a factor for visualization purposes. Dashed lines show the time interval that is affected by apodization.

(A color version of this figure is available in the online journal.)

that structures with larger ka should oscillate with larger periods. The wave modes excited in flux tubes by convection can, in principle, have a variety of wave numbers k. However, from the theory of the wave excitation (see for example Goldreich & Kumar 1990) one may argue that maximum of the excitation happens at wavelengths close to the local scale height in the atmosphere, providing that the modes with the wavelength about the tube radius ($\sim$250 km in our case) will have more power. This argument allows us to fix k and to speculate that, in principle, based on the work of Edwin & Roberts (1983), we can expect that magnetic structures with larger radius a would oscillate with

a larger period. Nevertheless, the strength of this dependence is difficult to estimate in our case, as one should know precisely the thermodynamic and magnetic parameters of the medium inside and outside the magnetic feature. In any case, the time-average size of the magnetic features we study in this Letter is approximately the same and, thus, the presence of characteristic oscillation modes would not explain the scatter in the temporal periods we observe between the different features. It will also be difficult to explain the abrupt change in the periods of the oscillation of a single feature and why some oscillations are damped while others are amplified. But more importantly, the

variations in the area we detect are so strong that, possibly, a nonlinear analysis of the variations is required, hence, the classical models are not suitable to explain these observations.

If they are not flux tube oscillation modes, the pattern we observe might be the forcing due to the evolution of the granules. Since the magnetic fields on the quiet Sun have mainly strengths lower than the equipartition field in the photosphere (∼300–500 G; see, e.g., Lin 1995; Khomenko et al. 2003; Martínez González et al. 2008; Orozco Suárez et al. 2007), the field lines are continuously buffeted by granular flows, being squashed or released everywhere and hence the magnetic fields are constantly being amplified or weakened. However, the present observations do not allow us to reject either scenario.

Now, an interesting question arises: do these waves propagate up through the solar atmosphere? We predict that, in case these waves propagate across the solar atmosphere, the very same phenomena reported in this Letter should be observed in the filter polarimeters on board the *Hinode* satellite. The different instruments on board the *Hinode* satellite provide valuable simultaneous data tracing the solar atmosphere (see, e.g., Martínez González & Bellot Rubio 2009). This data may be interesting to future work devoted to a detailed study of the propagation of these waves from the photosphere to the chromosphere. Wave propagation is an efficient means of carrying energy between different atmospheric heights and of dissipating it efficiently, mainly, through the formation of shocks. Therefore, we should put additional efforts into unveiling the role of this newly detected magnetic field oscillation in heating atmospheric layers.

REFERENCES

Barthol, P., et al. 2011, Sol. Phys., 268, 1
Bloomfield, D. S., McAteer, R. T. J., Mathioudakis, M., & Keenan, F. P. 2006, ApJ, 652, 812
Centeno, R., Collados, M., & Trujillo Bueno, J. 2009, ApJ, 692, 1211
Centeno, R., et al. 2007, ApJ, 666, 137L
Danilovic, S., et al. 2010, ApJ, 723, L149
De Moortel, I., Ireland, J., Hood, A. W., & Walsh, R. W. 2002, A&A, 387, L13
De Pontieu, B., Erdelyi, R., & de Wijn, A. G. 2003, ApJ, 595, L63
Edwin, P. M., & Roberts, B. 1983, Sol. Phys., 88, 179
Fujimura, D., & Tsuneta, S. 2009, ApJ, 702, 1443
Goldreich, P., & Kumar, P. 1990, ApJ, 363, 694
Gömöry, P., Beck, C., Balthasar, H., Rybák, J., Kucera, A., Koza, J., & Wöhl, H. 2010, A&A, 511, 14
Harvey, J. W., Branston, C. J., & Keller, C. U. 2007, ApJ, 659, L177
Jess, D. B., Mathioudakis, M., Erdélyi, R., Crockett, P. J., Keenan, F. P., & Christian, D. J. 2009, Science, 323, 1582
Khomenko, E. V., Collados, M., Solanki, S. K., Lagg, A., & Trujillo Bueno, J. 2003, A&A, 408, 1115
Krijger, J. M., Rutten, R. J., Lites, B. W., Straus, T., Shine, R. A., & Tarbell, T. D. 2001, A&A, 379, 1052
Lagg, A., et al. 2010, ApJ, 723, L164
Lin, H. 1995, ApJ, 446, 421
Lin, H., & Rimmele, T. 1999, ApJ, 514, 448
Lites, B. W., Rutten, R. J., & Kalkofen, W. 1993, ApJ, 414, 345
Lites, B. W., et al. 2008, ApJ, 672, 1237
Manso Sainz, R., Martínez González, M. J., & Asensio Ramos, A. 2010, A&A, submitted
Martin, S. F. 1988, Sol. Phys., 117, 243
Martínez González, M. J., & Bellot Rubio, L. 2009, ApJ, 700, 1391
Martínez González, M. J., Collados, M., Ruiz Cobo, B., & Beck, C. 2008, A&A, 477, 953
Martínez González, M. J., Collados, M., Ruiz Cobo, B., & Solanki, S. K. 2007, A&A, 469, 39
Martínez González, M. J., Manso Sainz, R., Asensio Ramos, A., & Bellot Rubio, L. 2010, ApJ, 714, L94
Martínez Pillet, V., et al. 2011, Sol. Phys., 268, 57
Orozco Suárez, D., Bellot Rubio, L. R., del Toro Iniesta, J. C., & Tsuneta, S. 2008, A&A, 481, 330
Orozco Suárez, D., et al. 2007, ApJ, 670, 61
Solanki, S. K., et al. 2010, ApJ, 723, L127
Stenflo, J. O., Solanki, S. K., & Harvey, J. W. 1987, A&A, 171, 305
Vecchio, A., Cauzzi, G., & Reardon, K. P. 2009, A&A, 494, 269
Wiegelmann, T., et al. 2010, ApJ, 723, L185